Computers and Chemical Engineering 169 (2023) 108078

Contents lists available at ScienceDirect

Computers and Chemical Engineering

journal homepage: www.elsevier.com/locate/compchemeng

Model-based energy management systems: Weighting of multiobjective functions using the Volatile Energy Prices Scalarization (VEPS)

Florian Fuhrmann *, Alexander Schirrer, Martin Kozek

Institute of Mechanics and Mechatronics, Technische Universität Wien, Getreidemarkt 9/BA, Wien 1060, Austria

ARTICLE INFO

Keywords:
Energy management system
Model predictive control
Multiobjective optimization
Mixed-integer linear programming
Thermal batch processes

ABSTRACT

Predictive energy management systems (EMSs) enable industrial plants to operate the energy supply systems at optimal efficiency, taking account of multiple objectives, including energy cost reduction. The performance of model-based EMSs depends on the appropriate design and correct scalarization of the resulting multiobjective function. This paper introduces the Volatile Energy Prices Scalarization (VEPS) method, which effectively designs, standardizes, and weighs the multiobjective function of model-based EMSs without the need for prior simulations or test runs. We present a case study, in which we compare the VEPS method to other state-of-the-art methods, utilizing a validated simulation model from an industrial food plant. The results show that the VEPS method outperforms other weighting methods with comparable tuning effort in this case-study. Moreover, the performance of the VEPS method is close to the Pareto-optimal performance. Economic weighting methods such as VEPS enable a fast and cost-effective implementation of EMS in the manufacturing industry.

1. Introduction

Decarbonization of industrial plants is a key measure of the European green deal. Energy management systems (EMS) that optimize the utilization of industrial energy supply systems (ESS) have therefore become increasingly important. EMS are usually optimization-based and have multiple objectives, often including energy cost reduction, emission reduction, and machine wear reduction. Multiobjective optimization (MOO) demands a suitable objective function design, and a method that takes account of the decision maker's preferences to ensure performance objectives are achieved (Marler and Arora, 2004).

Marler and Arora (2004) review different MOO concepts and distinguish between the a priori and a posteriori articulation of preferences by the decision-maker. A priori articulation of preferences means that the weighting of the different objectives is conducted before the optimization is executed, and where the weighted sum method is most commonly used. A posteriori articulation of preferences means that the MOO is executed with multiple weight settings, and the decision-maker compares performances to choose the preferred weights from a set of efficient solutions. It is commonly used for design optimization (Borghei and Ghassemi, 2020; Antipova et al., 2014; Karmellos and Mavrotas, 2019; Wu et al., 2016; Majewski et al., 2017; Sabio et al., 2012), process optimization (Sankar Parhi et al., 2020), and the combination of both applications (Maroufmashat et al., 2016; Samsatli and Samsatli, 2018; Zavala, 2013; Rangaiah et al., 2015), scheduling in manufacturing industries (Para et al., 2022; Zhou et al., 2018; Liu and Huang, 2014; Yuan Qian et al., 2020; Wang et al., 2016), supply chain management (Liu et al., 2014; Qiao et al., 2012), planning of oil spill responses (Zhong and You, 2011) sensor placement (Aghaei et al., 2015), or industrial water management (Boix et al., 2012; Vadenbo et al., 2014). The most common workflow for a posteriori articulation of preferences is to repeat the optimization with different objective weights and visualize the results in a Pareto front. The decision-maker can then choose the desired tradeoff between the objectives. This workflow has two significant drawbacks: The calculation time needed to construct a Pareto front with sufficiently high resolution, and the difficulty of interpreting the Pareto front for more than three dimensions (Copado-Méndez et al., 2014; Solanki et al., 2017; Schmitt et al., 2020).

Multiple methods have been devised to tackle these challenges. One solution is provided by methods for dimensionality reduction to reduce the number of objectives to a maximum of three (Copado-Méndez et al., 2014; Fonseca et al., 2020; Choi and Kwon, 2020; Zhang et al., 2020). Sabio et al. (2012) use principal component analysis to facilitate the interpretation and analysis of the possible solutions. The ε-constraint method converts multiobjective problems to single-objective problems by reformulating all but one objective as inequality constraints. The method is commonly used to facilitate the creation of the Pareto front

* Corresponding author.
E-mail address: florian.fuhrmann@tuwien.ac.at (F. Fuhrmann).

https://doi.org/10.1016/j.compchemeng.2022.108078
Received 17 May 2022; Received in revised form 3 August 2022; Accepted 24 November 2022
Available online 5 December 2022

Nomenclature

Abbreviations

BC	batch consumer
DoE	design of experiment
EMS	energy management system
ESS	energy supply system
HLC	higher-level control
HP	heat pump
LLC	low-level control
MILP	mixed-integer linear programing
MOO	multi objective optimization
MPC	model predictive control
OLP	online load predictor
PoU	Point of Utopia
SOC	state of charge
SOO	single objective optimization
SU	start-up
SD	shut-down
TES	thermal energy storage
VEPS	volatile energy price scalarization

Symbols

$\boldsymbol{C}$	cost coefficient vector in €
c	cost factor in e.g. €/MWh
E	power price in €/MWh
$\boldsymbol{F}$	vector of objective functions
J	weighed sum objective function
n	quantity
N_{P}	prediction horizon
P	power consumption
Q	weight factor
S	slack variable
t	time in h
t_{s}	sampling time in h
T	temperature
U	plant input
u	operation condition
v	start-up integer
w	shut-down integer

Indexes

avg	average
C	charge
D	discharge
full	full load
ineq	inequalities
eq	equalities
j	running index
l	running index
k	current time step
lhs	left hand side
lim	limit
min	minimum value
max	maximum value
out	outgoing mass flow
part	partial load
rhs	right hand side
std	scalarization
sink	heat sink of the heat pump
source	heat source of the heat pump

Further nomenclature

X	scalar variable
$\boldsymbol{X}$	vector variable
$\dot{X}$	time derivative of X
$\widehat{X}$	estimate of X
$\widetilde{X}$	normalization of X

(Marler and Arora, 2004; Karmellos and Mavrotas, 2019; Liu et al., 2014; Qiao et al., 2012; Fonseca et al., 2020; Choi and Kwon, 2020; Zhang et al., 2020).

Nevertheless, the high calculation times makes a posteriori articulation of preferences barely applicable for online methods such as model predictive control (MPC). As already mentioned, the weighted sum method is the most common approach to MOO with a priori articulation of preferences and is suitable for MPC (Marler and Arora, 2004). It reduces the computational effort by combining all objectives into one objective function to achieve online capability. The decision maker's preferences are incorporated by weighting the terms of the objective function by defining the weight parameters. There are multiple publications for EMS utilizing the weighted sum method (Schmitt et al., 2020; Hu et al., 2016; Hooshmand et al., 2013; Terlouw et al., 2019; Tan and Chen, 2020). The choice of weight parameters is crucial for the performance of the optimization and is a challenging task. There are several ways to obtain the weight parameters. As described for a posteriori articulation of preference, weighting can be chosen after creating a Pareto front with different weight settings (Choi and Kwon, 2020). However, constructing the Pareto front can be prohibitively expensive to compute and hard to interpret for more than three objectives (Marler and Arora, 2004; Schmitt et al., 2020). Schmitt et al. (2020) introduce an algorithm specifically to tackle this challenge.

The algorithm reduces the number of optimizations needed for creating the Pareto front and automatically selects a point in the Pareto front according to a predefined criterion (Schmitt et al., 2020). Using this method, the Pareto front for an MPC with two objectives and a prediction horizon N_{P} of 48 steps can be created in seconds. However, the authors state that the algorithm is limited in the number of objectives and number of steps for more complex applications (Schmitt et al., 2020).

The choice of weights utilizing Pareto fronts is time and resource-intensive, thereby increasing EMS implementation costs. Implementation cost is a main inhibitor for the broad application of model-based EMS. Moreover, ESS are often grown structures and are constantly undergo changes, hindering EMS's standardized integration (Fluch et al., 2017). A generic and straightforward implementation and weighting method is needed to reduce implementation costs.

Another challenge for the correct choice of the weight parameters is that the optimal solution according to the model is, in general, not optimal in real-world applications (Hutchison and Mitchell, 2008). During the development of optimization models for MPC, model-accuracy and complexity have to be balanced to obtain an appropriate model. The vast majority of publications investigating different methods for weighting MOO in EMS use the same models for optimization as for the evaluation of the optimality. There is a lack of literature investigating the effect of model accuracy on the choice of preferences in MOO. Schmitt et al. (2020) detect a general lack of research on the correct choice of weights for counteracting objectives.

This paper aims to close these research gaps with the following contributions:

- A straightforward and generically applicable objective function for EMS for thermal batch processes is introduced.

- The VEPS method is presented, which enables the a priori definition of weight parameters without creating a Pareto front.
- The performance of the presented VEPS method is compared to standard methods utilizing a validated detailed nonlinear model of an existing food plant.
- An investigation of the effect of model inaccuracy on the performance of EMS is conducted.

The EMS used in this publication is based on a generic component-based structure to enable a straightforward implementation (Fuhrmann et al., 2022a). Tests in the laboratory highlighted the importance of the choice of weights for the performance of the EMS (Fuhrmann et al., 2022b).

The VEPS method is based on a scalarization factor which enables an intuitive choice of weighting parameters. It is an application-oriented method developed for modular mixed integer linear program (MILP) based EMS for thermal batch production processes (Fuhrmann et al., 2022aa). It is important to note that validation with simulations shows high performance for the use case, a thermal batch production process, yet it is no general validation of the method. The VESP method eliminates the necessity of control experts to correctly define weight parameters and thereby reduces the implementation costs for EMS.

2. Methods

In this section, first basic definitions are given. Then the suggested objective function structure and the VEPS method are defined, followed by alternative weighting methods from the literature. Finally, the simulation study, including the simulation model, design of experiment (DoE), and the performance indicators are presented.

2.1. Basic definitions

Basic definitions for MOO, Pareto optimality, point of utopia (PoU), and the weighted sum formulation are given. For detailed descriptions and other literature, readers are referred to Marler and Arora (2004). Multiobjective optimization problems P_{MOO} are defined as follows:

$$\begin{aligned} P_{\mathrm{MOO}} : &\min \boldsymbol{F}(\mathbf{x}) = \left(F_1(\mathbf{x}), F_2(\mathbf{x}), \dots, F_{n_{\mathrm{obj}}}(\mathbf{x})\right) \\ &\text{s.t} \quad g_j(\mathbf{x}) \leq 0,\ j = 1, 2, \dots, n_{\mathrm{ineq}} \\ &\qquad h_l(\mathbf{x}) = 0,\ l = 1, 2, \dots, n_{\mathrm{eq}} \end{aligned} \tag{1}$$

where $\boldsymbol{F}$ is a vector of n_{obj} objective functions, $\mathbf{x} \in \mathbf{X}$ is a vector of decision variables, n_{ineq} is the number of inequality constraints and n_{eq} is the number of equality constraints. In general, no single global solution other than a Pareto front $\mathbf{X}^*$ of *Pareto optimal* solutions $\mathbf{x}^*$ exists. A point, $\mathbf{x}^* \in \mathbf{X}$, is Pareto optimal if there is no other point, $\mathbf{x} \in \mathbf{X}$, such that $\boldsymbol{F}(\mathbf{x}) \leq \boldsymbol{F}(\mathbf{x}^*)$ where $\leq$ is understood element-wise and $F_i(\mathbf{x}) < F_i(\mathbf{x}^*)$ for at least one function.

The PoU is defined by

$$\begin{aligned} \boldsymbol{F}^{\mathrm{Utopia}} &= \left(F_1^{\mathrm{Utopia}}, F_2^{\mathrm{Utopia}}, \dots, F_{n_{\mathrm{obj}}}^{\mathrm{Utopia}}\right) \\ F_i^{\mathrm{Utopia}} &= \min F_i(\mathbf{x}) \end{aligned} \tag{2}$$

Thereby, the PoU is the optimal point in respect to each objective function and in general unattainable. The weighted sum method is defined as:

$$J = \sum_{i=1}^{n} \boldsymbol{Q}_i \cdot \boldsymbol{F}_i(\mathbf{x}) \tag{3}$$

where J is the objective function, and $\boldsymbol{Q}$ is a vector of weight parameters. In the following section, a practical structure for the definition of $\boldsymbol{F}$ and the choice of the weight parameters $\boldsymbol{Q}$ are given.

2.2. Suggested objective function structure

The objective function structure presented in this paper was developed on the basis of the EMS presented in Fuhrmann et al. (2022a). The EMS consists of a higher-level controller (HLC), a lower-level controller (LLC), and an online load predictor (OLP) and is displayed in Fig. 1. The HLC and LLC both use a modular mixed-integer linear program (MILP) optimization formulation. A MILP-optimization problem is built up from inputs, a set of constraints, and an objective function defined component-wise. This structure enables a generic application of the EMS on various ESS of different industrial plants. A detailed description of the constraints and parameters of the components used in the case study can be found in Fuhrmann et al. (2022a). In the current paper, the focus is laid on the objective function of the EMS.

All optimization-based EMS require an objective function J describing the optimal operation of the ESS. The vast majority of objective functions minimize a set of M cost terms, which are a product of cost factors C_m and the corresponding weighting factor Q_m:

$$J = \min \sum_{j=k}^{k+N_{\mathrm{P}}-1} \sum_{m=1}^{M} C_{j,m} \cdot Q_m \tag{4}$$

where k is the current time-step and N_{P} is the control horizon. The cost factors C represent operation optimization objectives, such as electric power costs or machine wear, and objectives concerning control performance, such as trajectory costs or plant input variation costs. As mentioned above, the MILP formulation defined in Fuhrmann et al. (2022a) enables a component-wise definition of J similar to (Moser et al., 2020).

$$J = \sum_{n=1}^{N} J_{\mathrm{Comp},n} \tag{5}$$

$$J_{\mathrm{Comp},n} = \sum_{j=k}^{k+N_{\mathrm{P}}-1} \sum_{m=1}^{M_n} C_{j,m,n} \cdot Q_{m,n} \tag{6}$$

where N is the number of components, M_n is the number of cost factors considered for a component, and the costs are summed up for the prediction horizon $\mathrm{N_P}$. In (6), the high number and importance of the weighting parameters $Q_{m,n}$ becomes apparent as it decides which component and cost factor is considered while optimizing.

2.2.1. Cost factors

In this section, the cost factors C_m which are used in the case study are presented. First, the control-specific terms are defined, followed by the operation optimization terms.

Plant input deviation. To smoothen the plant input for wear reduction, the plant input deviation is penalized by the cost factor $C_{j,\Delta U}$ defined as:

$$C_{j,\Delta\mathrm{U}} = abs\left(\boldsymbol{U}_{j+1} - \boldsymbol{U}_j\right) \tag{7}$$

where $\boldsymbol{U}$ is the vector plant inputs restricted to values from 0 to 1. Note

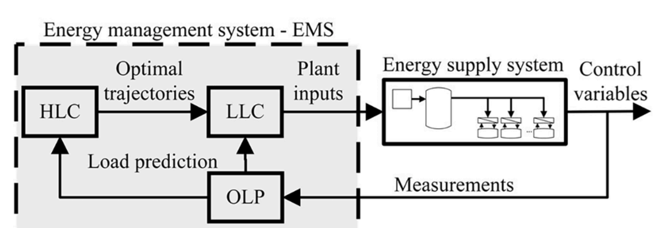

Fig. 1. Architecture of the energy management system (EMS) including the higher level controller (HLC), the lower level controller (LLC) and the online load predictor (OLP). Adapted from Fuhrmann et al. (2022a).

that absolute values in the objective function must be reformulated to retain linearity. One linearization method is displayed in (8) (Chan et al., 2022).

$$abs(X) = X' \Leftrightarrow \begin{cases} X \leq X' \\ -X \leq X' \end{cases} \tag{8}$$

Trajectory deviation. The trajectory deviation cost factor $C_{j,traj}$ evaluates deviations of the plant input from a given optimal trajectory $\boldsymbol{U}_{traj}$ and is defined as:

$$C_{j,\text{traj}} = abs\left(\boldsymbol{U}_j - \boldsymbol{U}_{j,traj}\right) \tag{9}$$

Note again that a linear reformulation is required. Optimal trajectories $\boldsymbol{U}_{traj}$ are often used in multi-layer optimization where $\boldsymbol{U}_{traj}$ is calculated by the HLC and used as an input for the LLC.

Slack constraint. Slack or soft constraints are used to avoid undesired system conditions at all costs and avoid infeasibility by numerical violations of constraints (Fuhrmann et al., 2020a). The working principle is that a slack variable $\boldsymbol{S}$ is introduced to quantify the violation of a constraint regarding state $\boldsymbol{X}$.

$$C_{j,\text{S}} = \boldsymbol{S}_j \tag{10}$$

with the constraints:

$$\begin{aligned} &\boldsymbol{X} - \boldsymbol{S} \leq \boldsymbol{X}_{\max} \\ &\boldsymbol{X} + \boldsymbol{S} \geq \boldsymbol{X}_{\min} \\ &\boldsymbol{S} \geq 0 \end{aligned} \tag{11}$$

where $\boldsymbol{S}$ is the vector of the slack variable and $\boldsymbol{X}$ is the vector of the state variable.

Electric power cost. The electric power cost factor is driven by the electric power consumption of a component. As the power consumption $\boldsymbol{P}$ is usually given in power (kW), it has to be multiplied by the sampling time t_C as stated in (12):

$$C_{j,\text{power}} = \boldsymbol{P}_j \cdot t_\text{C} \tag{12}$$

where $\boldsymbol{P}$ is the electric power consumption of the j-th component.

Start-up cost & shut-down cost. The start-up and shut-down cost factors are defined by the occasion of a start-up or shut-down event:

$$C_{j,\text{SU}} = \boldsymbol{v}_j \tag{13}$$

$$C_{j,\text{SD}} = \boldsymbol{w}_j \tag{14}$$

where $\boldsymbol{v}$ is a vector of integers indicating start-up events with a value of 1 and $\boldsymbol{w}$ is a vector of integers indicating shut-down events with a value of 1.

Further cost factors. Further possible cost factors are, among others, the CO_2-emissions C_{CO_2}, power-independent operation cost C_opex, power-peak costs C_peak, operator costs C_operator.

2.2.2. VEPS method

The definitions in Section 2.2.1 show that the cost factors C can have different magnitudes. To enable multiobjective optimization, scalarization and a correct weighting of each cost factor of the objective function J is necessary (Marler and Arora, 2004). Therefore, the choice of weighting factors Q is crucial to the performance of the EMS. This section presents the VEPS method for the efficient scalarization choice of $Q_{m,n}$ for an objective function J of the structure presented in (2)-(3). The VEPS method consists of tuning parameters which are comprehensible, meaningful and clear to operators or technicians handling an ESS. In this way, the resource intensive parameter tuning by experts or experiments (Fonseca et al., 2020) and suboptimal standard weight tunings, e.g. all weights equal to one (Hu et al., 2016), are avoided. Furthermore, a reasonable solution space regarding production and system constraints can easily be defined.

First, a scalarization factor based on volatile energy prices is defined. After that, weighting rules utilizing this scalarization factor are presented for the cost factors given in Section 2.2.1.

Scalarization factor. The volatile energy price-based scalarization factor enables an intuitive balancing of different, partly conflicting objectives. The cost of a start-up event has to be set in meaningful relation to power cost savings. Economic factors are the primary concern for plant operators, and the power costs are vivid values to operators. Therefore, potential power cost savings are used to normalize the different cost terms. In addition, the scalarization factor avoids numerical problems by ensuring that all terms of the cost function have the same magnitude, except for the slack constraint for which a different magnitude is desired.

Under the twin assumptions of a fixed production plan and no possible energy carrier substitution, only storage management can be used for time shifts of the power consumption. The reduction of the power costs term is thereby dependent on the fluctuation of the power price $\boldsymbol{E}$.The average power price difference between two time-steps is a simple but suitable quantification of the power price fluctuation and is therefore utilized for scalarization.

$$c_\text{std} = \sum_{j=1}^{N_\text{P}} \frac{\sqrt{\left(\boldsymbol{E}_{j+1} - \boldsymbol{E}_j\right)^2}}{N_\text{P}} \cdot P_\text{max}, \tag{15}$$

where c_std is the scalarization factor and P_max is the maximum power consumption of the ESS in one time-step.

Plant input deviation. A rule for normalizing the cost factor for the deviation of the plant input $Q_{\Delta\text{U}}$ with the power costs is given in (16) where ΔU_max is the maximum desired deviation of U in one control step. The deviation of the plant input is defined as $\Delta U_j = abs(U_{j+1} - U_j)$ (compare (7)), and therefore is restricted to values from 0 to 1. For components where the performance is not influenced by changes of the working point ΔU_max can be set to the largest possible value of 1. For components sensitive to changes of the plant input lower values should be chosen for ΔU_max. Values for ΔU_max can often be derived from component manuals.

$$Q_{\Delta\text{U}} = c_\text{std} \cdot (1 - \Delta U_\text{max}) \tag{16}$$

Thereby, in case $\Delta U_\text{max} = 1$, where changes of the plant input have no influence on the performance of the EMS, $Q_{\Delta\text{U}}$ is zero and the plant input deviation does not contribute to the cost function. In the case of low ΔU_max the cost factor is close to the scalarization factor. Ramp constraints are a common alternative means of prohibiting undesired changes of $\boldsymbol{U}$. A definition of ramp constraints can be found in Fuhrmann et al. (2022a).

Trajectory deviation. The trajectory deviation term evaluates the deviation of the plant inputs from their trajectory. The weighting factor Q_traj normalizes the term by utilizing a desired maximum deviation of the plant input $\boldsymbol{U}_\text{HP}$ from the trajectory $\Delta U_\text{traj,max}$.

$$Q_\text{traj} = \frac{c_\text{std}}{\Delta U_\text{traj,max}} \tag{17}$$

Thereby, Q_traj increases strongly when even small deviations from the trajectory are undesired. The minimum value of Q_traj is c_std as even in case large deviations are acceptable, a trajectory following is always desired in a two-layer EMS.

Slack constraint. Even though slack constraints are part of the objective function they are still constraints and violations should be avoided whenever possible. Therefore, the slack cost term Q_S should exceed all other costs factors. Previous investigations of the authors showed that it is a useful choice to define Q_S three magnitudes higher than all other cost terms (Fuhrmann et al., 2020b). The weighting includes the magnitude of undesired changes of the constrained state S_{std} which can be defined without simulations.

$$Q_S = 10^3 \cdot \frac{c_{std}}{S_{std}} \tag{18}$$

Electric power cost. The electric power cost can be weighted straightforwardly with the power price $\boldsymbol{E}$, as they are used for the scalarization:

$$Q_{power} = \boldsymbol{E}_j \tag{19}$$

Start-up cost & shut-down cost. The weight of a start-up process Q_{SU} and shut-down process Q_{SD} are calculated with a desired minimal duration of a condition $t_{SU,\ desired}$ and $t_{SD,\ desired}$ as these parameters are intuitive for operators. Too short running or standstill durations typically lead to ineffective operation and high machine wear. This objective should not be mixed up with the minimum uptime in steps $\boldsymbol{n}_{HP,\ up}$, which can be implemented as a hard constraint.

$$\begin{aligned} Q_{SU} &= c_{std} \cdot t_{SU,desired} \\ Q_{SD} &= c_{std} \cdot t_{SD,desired} \end{aligned} \tag{20}$$

Thereby, Q_{SU} and Q_{SD} are zero when no minimal up- or downtime is required.

2.3. Simulation study

In the simulation study, the influence of changes in the objective function on the performance of the EMS was investigated for an industrial food plant. Simulation models of the industrial plant used in Fuhrmann et al. (2022a) and validated with industrial measurement data (Sack, 2021) were utilized. The industrial plant manufactures meat products that undergo specific temperature trajectories to alter the meat's taste and structure and extend the expiration date. The structure and basic data of the components are displayed in Fig. 2. Main heat supply unit of the industrial plant is a heat pump (HP) with 0.206 MW maximum heat flow at the heat sink, which utilizes a constantly available heat recovery system as heat source. A thermal energy storage (TES) with 12.7m^3 volume ensures production safety and enables flexibility in the power consumption. Four heat exchangers are used to supply the peak-like demand of four production units. These batch consumers (BC) have a maximum short term heat demand of 1.367 MW.

The simulation model of the plant has a high level of detail and considers nonlinear effects like liquid-mixing, underlying controllers, phase changes, or temperature gradient dependent effects. The model was developed component-wise utilizing Dymola® and Matlab Simulink®. A validation and further description of the model is published in Fuhrmann et al. (2022a), Sack (2021).

The EMS uses a component-wise MILP-formulation of the plant as a basis for the optimization. These formulations were published in detail in Fuhrmann et al. (2022a).

MATLAB Simulink® was used as a simulation platform. For each time-step, the simulation model was used to simulate the plant behavior with the inputs determined by the EMS. The plant states of the simulation model were used as measurements for the EMS optimization. A single simulation spans one month of production using measurement data from 102 heat treatments as a production plan.

A crucial difference to the existing literature consists in considering the impact of weight settings on the optimization performance where another more detailed simulation model is utilized to quantify the controller performance rather than the optimization model itself. In contrast to the optimization models used in the EMS, the simulation model is nonlinear and has a high level of detail. For example, the simulation model of the heat pump takes account, among other effects, of the underlying internal PID-controller, nonlinear characteristic curves of valves, and nonlinear fluid properties.

2.3.1. Design of experiment

It is the goal of the simulation study to compare the EMS-performance under weight settings defined by the VEPS-method with alternate weight settings. Two approaches were used to create alternate weight settings for the three weights $Q_{\Delta U}$,Q_{power}, Q_{SU}. First, alternative weighting methods were taken from literature. These methods are described in Section 2.3.3. Second, random deviations of the weight parameters defined by the VEPS factor were investigated. The deviation of parameters was executed by multiplying each weight parameter with a deviation factor D ranging from 10^{-4} to 10^4 as described in (21):

$$\begin{aligned} &Q_{m,deviated} = Q_{m,VEPS} \cdot D_m \\ &\textit{with} \\ &D_m \in \left[10^{-4}, 10^{-3}, 10^{-2}, 0.04, 10^{-1}, 0.25, 0.5, 1, 2, 4, 10, 25, 10^2, 10^3, 10^4\right] \end{aligned} \tag{21}$$

These deviations also enable a discussion on the effect of enlarging or decreasing a certain weight factor, thus constituting a sensitivity analysis with respect to the weight factors. All possible combinations of weighting factors were simulated.

2.3.2. Performance evaluation

The performance of the weighting and scalarization methods was evaluated in all simulations taking account of the three performance indicators:

1. Count of violations of the desired maximum deviation of the plant input $N_{\Delta U_{max}}$
2. Number of short start-up events $N_{short\ SU}$
3. Total energy costs C_{energy},

These three performance indicators are normalized to enable a clear and intuitive assessment of the results and render the results of different simulation studies comparable. The normalization of all performance

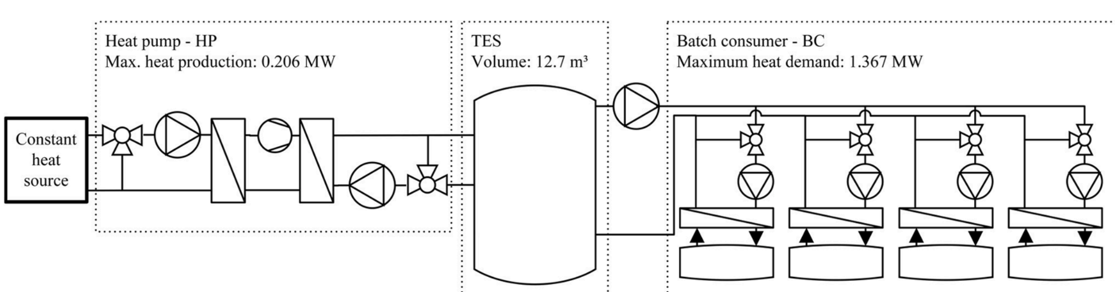

Fig. 2. Structure of the food production plant considered in the simulation study consisting of a constant heat source, a heat pump (HP), a thermal energy storage (TES) and four batch consumers (BC). Adapted from Fuhrmann et al. (2022a).

indicators follows the formula:

$$\tilde{I}_n = \frac{I_n - I_{\min}}{I_{\max} - I_{\min}} \textit{ with}$$

$$I_{\min} = \min(I_1, I_2, \ldots, I_N) \tag{22}$$

$$I_{\max} = \max(I_1, I_2, \ldots, I_N)$$

where I_n is the performance indicator of the *n*-th simulation, N the total number of experiments, and $\tilde{I}$ the normalized performance indicator. Thereby, $\tilde{I}$ has a value of 0 for the best performance and 1 for the worst performance.

2.3.3. Compared weighting methods

The performance of the VEPS method was compared to two common alternative a priori weighting methods and the most common a posteriori weighting method.

For the two a priori methods, the terms of the objective function were scalarized by dividing them through the maximum value of the term.

$$C_i = 1/C_{i,\max} \tag{23}$$

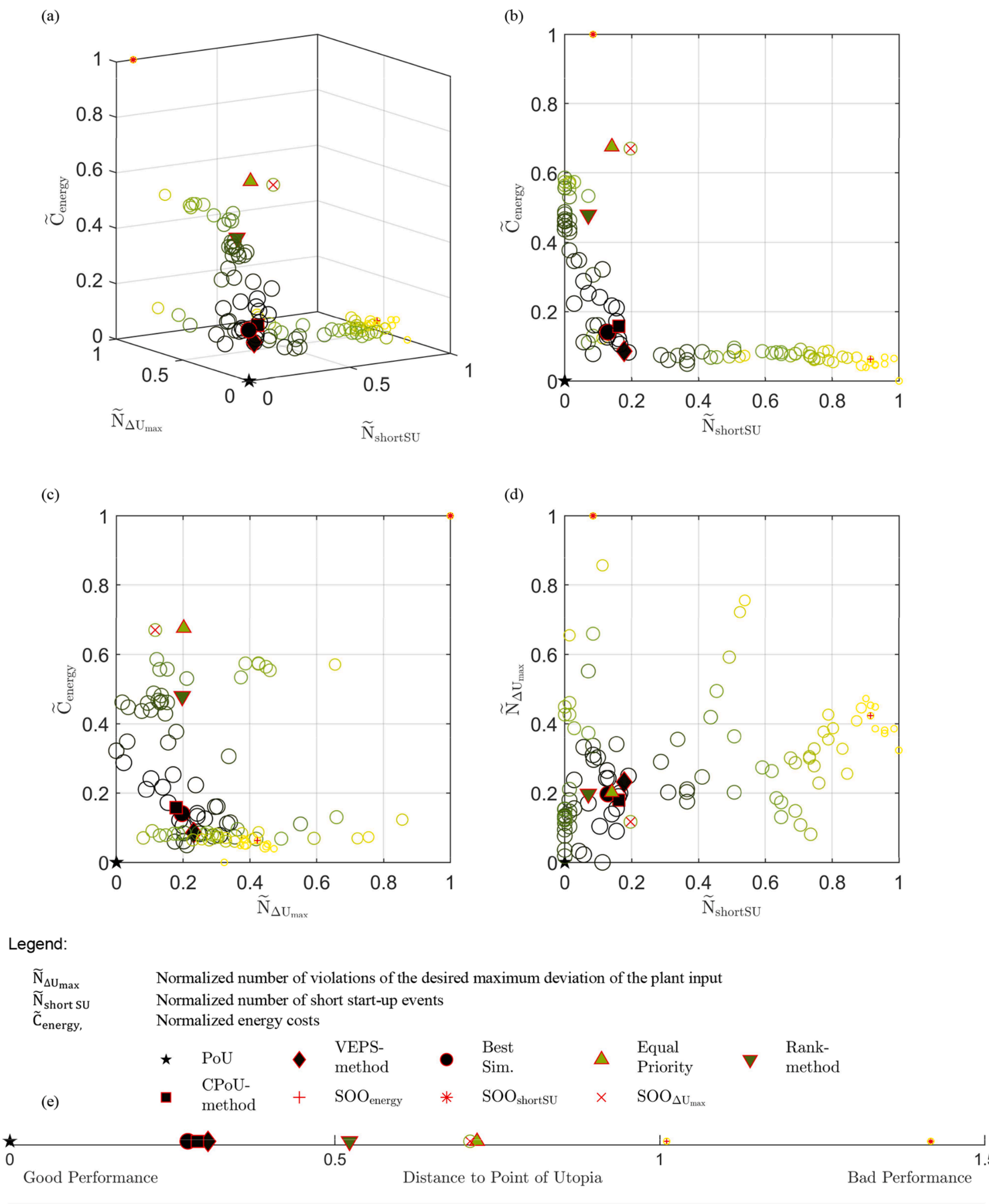

Fig. 3. a–e: Performance validation for all executed simulations. The Point of Utopia (PoU) and the results with specific settings are marked as described in the legend above. All other simulation results are marked by circles. To enhance readability the performance is also indicated by color and size of the markers, where big black markers indicate good performances and small yellow markers indicate bad performances, using the distance to PoU as indicator.

The first alternative method is the ranking method, in which the various objectives are ranked by importance and weighted accordingly (Marler and Arora, 2004). For the simulation, the power costs were chosen with the highest priority $Q_{power} = 3$, start-up events as medium priority $Q_{SU} = 2$, and aggressiveness of the controller as lower priority $Q_{\Delta U} = 1$. As a second method, all weights were set to a value of one, which is an extremely simple but still common method (Hu et al., 2016).

As a posteriori method, the optimization closest to the PoU (CPoU) was chosen (Schmitt et al., 2020).

3. Results

The performance of all executed simulations visualized in Fig. 3a–e. The weight settings and performance indicators of the VEPS method, the comparison method, the best performance, and the three single objective optimization (SOO) runs are listed in Table 1. In the remainder of this section, first, the performance of the VEPS method is compared to the methods described in the literature. Next, the sensitivity of the weight parameters is analyzed, and finally, the impact of the optimization model on the optimization performance is discussed.

3.1. Comparison of the weighting methods

Fig. 3(a–e) and Table 1 compare the different weighting methods. In Fig. 3(a–d), the normalized performance validation indicators $\widetilde{N}_{\Delta U_{max}}$, $\widetilde{N}_{short\ SU}$ and $\widetilde{C}_{energy}$ are plotted on the axes. Based on the normalization described in Section 2.3.2., the best performance is indicated by a value of zero and the worst with a value of one. The closer a performance is to the origin - the PoU - the better the performance is rated. To improve the readability of the 3D plot, the size and color of each marker are a function of the distance to the PoU. The closer a performance is to the PoU, the darker and bigger the marker is displayed.

For the first comparison of methods, the focus was put on the distance to PoU displayed in Fig. 3(e) and listed in the last column of Table 1. The simulation closest to the PoU, the simulation using the VEPS method, and the alternative using the CPoU-method displayed similar overall performance. Compared to the solution closest to PoU, the VEPS method overweighs the power cost by a factor of two. On the one hand, this causes a slightly more aggressive controller and 38.0% more short SU events. On the other hand, the power costs are reduced by 38.6%.

The alternative CPoU has a tenfold weight on ΔU, causing a strongly reduced aggressiveness of the controller, which is bought with 26% more startup events and 12% higher energy cost than the simulation closest to PoU. The alternative using a posteriori articulation shows the best result of all investigated rules. It is important to note that the CPoU is an a posteriori articulation of preferences demanding the high burden of creating the Pareto front before defining the weights. Still, it is further proof that a posteriori methods utilizing the Pareto front lead to a well-balanced objective function.

The ranking method and the equal-weights method produced results far from the optimum and significantly worse than the VEPS method. The distance to the point of utopia is about two times the distance of the best performance. This is mainly caused by high energy costs. The reason is clearly that the scalarization based on the maximum value caused the weight to be two magnitudes from the optimal value. A more sophisticated economic weighting such as the VEPS method is needed to achieve acceptable performance with a priori articulation of preferences.

3.2. Discussion of model inaccuracies

The simulations considering single objectives give interesting insights into the impact of inaccuracies of the optimization model on the optimization result. It is remarkable that no SOO simulation achieved the best result in the considered objective even though this would be expected. This is due to inaccuracies of the optimization model. The SOO for energy cost is closest to the minimal energy cost. Nevertheless, the optimization model does not take account of the fact that changes of the HP's working point cause an efficiency reduction.

For the other two objectives, reducing $N_{short\ SU}$ and $N_{\Delta Umax}$ the effect is even stronger. Here, in addition to model inaccuracies, the definition of $C_{\Delta U}$ displayed in (7) has a strong influence. The cost term $C_{\Delta U}$ is the absolute sum of differences of the plant input vector U. This definition includes shut-down and start-up maneuvers. Thereby the weight $Q_{\Delta U}$ has direct influence on the performance indicator $N_{short\ SU}$ .The effect becomes clearly visible in Fig. 3d, where no classical Pareto front is visible. Instead, many results are close to the PoU because there is no classical tradeoff between reducing $N_{short\ SU}$ and $N_{\Delta Umax}$. However, these points are far from the PoU as the energy costs increase strongly when the HP is operated in constantly also on times of high power prices. The HP operation has to be aggressive enough to follow the volatile energy prices. Therefore, the VEPS method is an effective method to weight the objectives of an EMS in respect of volatile energy prices.

3.3. Parameter sensitivity

Fig. 4(a–c) shows the sensitivity of control performance to changes in the weighting parameters. Each graph shows the performance of simulations where all but one weighting parameter was frozen. The remaining weighting parameter was changed from 10^{-4} to 10^{4}. All three graphs show that the VEPS method effectively calculates weighting parameters in the sensitive range. In general, the parameters are sensitive in a range of $0.01 < D < 100$. Thereby, the VEPS method can be used as a starting point to investigate different solution spaces. Fig. 4(a) indicates that increasing the $Q_{SU\ short}$ parameter would reduce the number of starting events while increasing both the number ΔU_{max} violations and the energy cost. The weight of the VEPS method seems to be chosen correctly, as a slight reduction of the weight would cause a substantial increase in the short starting maneuvers.

In Fig. 4(b), it can be seen that $C_{\Delta U}$ includes the switching maneuvers as the changes in $N_{short\ SU}$ and $N_{\Delta Umax}$ are strongly correlated. An increase of $Q_{\Delta U}$ would cause rising energy costs and therefore, again, the VEPS method has led to a meaningful weight parameter choice according to this plot.

Fig. 4(c) again shows the result already displayed in Section 3.1: For

Table 1

Results of chosen simulations. $\widetilde{Q}$ are weight parameters normalized by the weight closest to PoU.

Name	$\widetilde{Q}_{\Delta U}$	$\widetilde{Q}_{SU}$	$\widetilde{Q}_{power}$	$\widetilde{N}_{\Delta U_{max}}$	$\widetilde{N}_{short\ SU}$	$\widetilde{C}_{energy}$	Distance to PoU	Relative Distance to PoU
Best Simulation	1	1	1	0.197	0.129	0.140	0.274	1
VEPS method	0.5	0.5	1	0.232	0.178	0.086	0.305	1.11
Equal priority method	0.677	0.025	0.007	0.202	0.141	0.675	0.719	2.62
Ranking method	0.677	0.049	0.022	0.197	0.070	0.480	0.523	1.91
CPoU-method	5	0.5	1	0.179	0.162	0.157	0.288	1.05
SOO for energy cost	0	0	0.5	0.423	0.916	0.063	1.010	3.67
SOO for ΔU	0.5	0	0	0.117	0.197	0.670	0.708	2,58
SOO for short start up	0	0.5	0	1	0.085	1	1.417	5.17

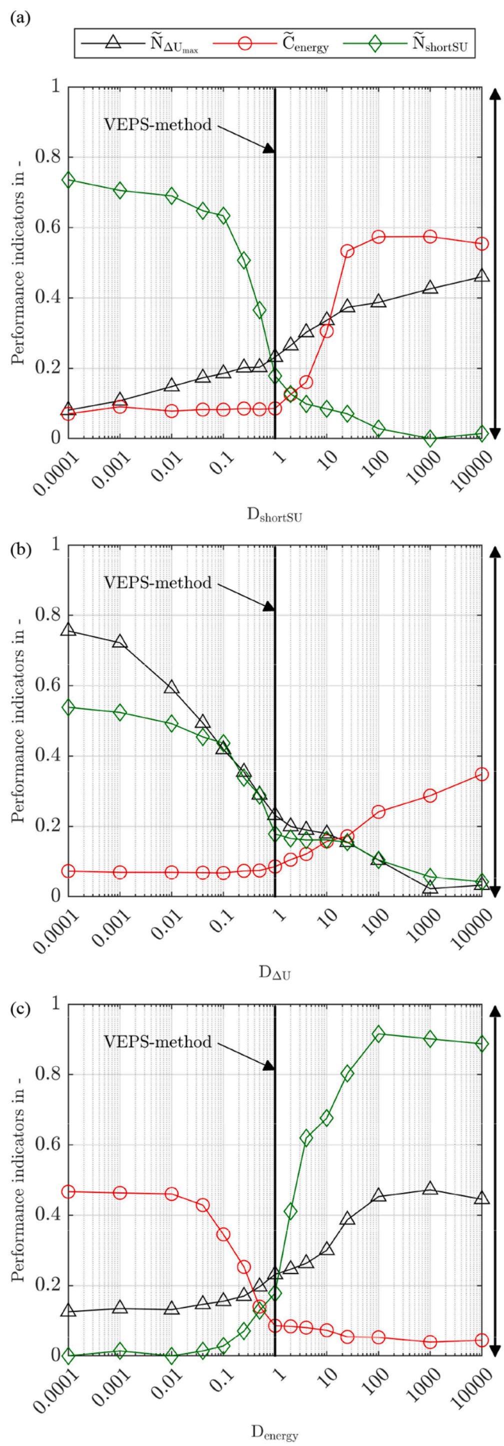

Fig. 4. a–c Parameter sensitivity for changes in three weight parameters.

this use case, the VEPS method weighs strongly on energy cost, and the weight is close to the upper end of the sensitive area. The best result is visible in this plot at $D_{energy} = 0.5$. An increasing weight on energy cost would substantially increase both undesired intense changes in the plant input and a high number of starting maneuvers.

4. Conclusion

This paper has proposed and characterized the VEPS method for weighting multiobjective functions for EMSs considering volatile energy prices. The effectiveness of the VEPS method is successfully demonstrated in a case study considering an existing food processing plant. The performance of the method is compared with existing methods from literature. The results show that for the investigated use-case, the VESP-method outperforms all other considered methods with an a priori articulation of the decision maker's preferences. Moreover, the performance is similar to the a posteriori method CPoU and close to the performance closest to the point of utopia. Further case studies with different systems are needed to verify the effectiveness of the method for other areas.

The VEPS method does not require to conduct elaborate simulation studies, calculating the Pareto front, or numerous test runs to define the weight parameters. In addition, the definition of the weight parameters enables intuitive weighting even for inexperienced plant operators. The implementation costs are thus reduced, and the applicability of EMS in the manufacturing industry is increased. Furthermore, the VEPS method results in weight parameters sensitive to changes, facilitating subsequent changes to them.

The case study also confirmed that methods using the Pareto front for a posteriori articulation of the decision maker's preferences lead to good results. Nevertheless, computing and visualizing Pareto fronts with more than three dimensions is challenging. Therefore, economic a priori methods such as the VEPS method are more useful for the fast and cost-effective implementation of EMS in the manufacturing industries. The simulation study validates the VEPS method for manufacturing plants with thermal batch processes. General validation of the method requires results for other processes or analytical verification.

CRediT authorship contribution statement

Florian Fuhrmann: Conceptualization, Methodology, Validation, Investigation, Writing – original draft, Visualization. **Alexander Schirrer:** Supervision, Conceptualization, Methodology, Writing – review & editing. **Martin Kozek:** Project administration, Funding acquisition, Writing – review & editing.

Declaration of Competing Interest

The authors declare that they have no known competing financial interests or personal relationships that could have appeared to influence the work reported in this paper.

Acknowledgements

The authors acknowledge TU Wien Bibliothek for the financial support offered through its Open Access Funding Program and for editing/proofreading. This work was supported by the projects ‘EDCSproof’ and ‘Industry4Redispatch, which are part of the energy model region NEFI - New Energy for Industry and are funded by the Austrian Climate and Energy Fund [FFG, No. 868837 & 887780].

References

Aghaei, J., Baharvandi, A., Rabiee, A., Akbari, M.A., 2015. Probabilistic PMU Placement in electric power networks: an MILP-based multiobjective model. IEEE Trans. Ind. Inform. 11 (2), 332–341.

Antipova, E., Boer, D., Guillén-Gosálbez, G., Cabeza, L.F., Jiménez, L., 2014. Multi-objective optimization coupled with life cycle assessment for retrofitting buildings. Energy Build. 82, 92–99.

Boix, M., Montastruc, L., Pibouleau, L., Azzaro-Pantel, C., Domenech, S., 2012. Industrial water management by multiobjective optimization: from individual to collective solution through eco-industrial parks. J. Clean. Prod. 22 (1), 85–97.

Borghei, M., Ghassemi, M., 2020. A multi-objective optimization scheme for resilient, cost-effective planning of microgrids. IEEE Access 8, 206325–206341.

Chan, M., Yin, Y., Amada, B., Wiliams, P., Xiao, D. 2022 December 05. “Optimization with absolute values,” *Cornell University Computational Optimization Open Textbook*. Available: https://optimization.cbe.cornell.edu/index.php?title=Optimization_with_absolute_values.

Choi, H.K., Kwon, J.S.I., 2020. Multiscale modeling and multiobjective control of wood fiber morphology in batch pulp digester. AIChE J. 66 (7), 1–13.

Copado-Méndez, P.J., Guillén-Gosálbez, G., Jiménez, L., 2014. MILP-based decomposition algorithm for dimensionality reduction in multi-objective optimization: application to environmental and systems biology problems. Comput. Chem. Eng. 67, 137–147.

Fluch, J., et al., 2017. Evaluation of innovative integration concepts of combined solar thermal and heat pump systems for efficient thermal supply of industrial processes. In: Proceedings of the EuroSun 2016, pp. 1–13.

Fonseca, J.D., Latifi, A.M., Orjuela, A., Rodríguez, G., Gil, I.D., 2020. Modeling, analysis and multi-objective optimization of an industrial batch process for the production of tributyl citrate. Comput. Chem. Eng. 132, 106603 https://doi.org/10.1016/j.compchemeng.2019.106603.

Fuhrmann, F., Schirrer, A., Kozek, M., 2020a. MPC for process heat supply systems : considering load prediction uncertainty caused by human operators. In: Proceedings of the 30th European Symposium on Computer Aided Chemical Engineering (ESCAPE30). Milano, Italy, p. 2020. *May 24-27*.

Fuhrmann, F., Schirrer, A., Kozek, M., 2020b. MPC for Process heat supply systems: considering load prediction uncertainty caused by human operators. Comput. Aided Chem. Eng. 48, 1219–1224.

Fuhrmann, F., Kozek, M., Schirrer, A., 2022a. Model-predictive energy management system for thermal batch production processes using online load prediction. Comput. Chem. Eng. 163 (107830).

Fuhrmann, F., Windholz, B., Schirrer, A., Schenzel, K., Knöttner, S., Kozek, M., 2022b. Energy management for thermal batch processes with temporarily available energy sources–Laboratory experiments. Case Stud. Therm. Eng. 39, 102473.

Hooshmand, A., Asghari, B., Sharma, R., 2013. A novel cost-aware multi-objective energy management method for microgrids. In: Proceedings of the IEEE PES Innovative Smart Grid Technologies Conference ISGT, pp. 1–6.

Hu, Z., et al., 2016. Multi-objective energy management optimization and parameter sizing for proton exchange membrane hybrid fuel cell vehicles. Energy Convers. Manag. 129, 108–121.

D. Hutchison and J.C. Mitchell, *Multiobjective optimization: interactive and evolutionary approaches*, vol. 5252 LNCS. 2008.

Karmellos, M., Mavrotas, G., 2019. Multi-objective optimization and comparison framework for the design of distributed energy systems. Energy Convers. Manag. 180 (September 2018), 473–495.

Liu, C.H., Huang, D.H., 2014. Reduction of power consumption and carbon footprints by applying multi-objective optimisation via genetic algorithms. Int. J. Prod. Res. 52 (2), 337–352.

Liu, Z., Qiu, T., Chen, B., 2014. A study of the LCA based biofuel supply chain multi-objective optimization model with multi-conversion paths in China. Appl. Energy 126 (2014), 221–234.

Majewski, D.E., Wirtz, M., Lampe, M., Bardow, A., 2017. Robust multi-objective optimization for sustainable design of distributed energy supply systems. Comput. Chem. Eng. 102, 26–39.

Marler, R.T., Arora, J.S., 2004. Survey of multi-objective optimization methods for engineering. Struct. Multidiscip. Optim. 26 (6), 369–395.

Maroufmashat, A., Sattari, S., Roshandel, R., Fowler, M., Elkamel, A., 2016. Multi-objective optimization for design and operation of distributed energy systems through the multi-energy hub network approach. Ind. Eng. Chem. Res. 55 (33), 8950–8966.

Moser, A., et al., 2020. A MILP-based modular energy management system for urban multi-energy systems: performance and sensitivity analysis. Appl. Energy 261, 114342. https://doi.org/10.1016/j.apenergy.2019.114342.

Para, J., Del Ser, J., Nebro, A.J., 2022. Energy-aware multi-objective job shop scheduling optimization with metaheuristics in manufacturing industries: a critical survey, results, and perspectives. Appl. Sci. 12 (3).

Qiao, Z., Wang, Z., Zhang, C., Yuan, S., Zhu, Y., Wang, J., 2012. Optimal design of sustainable cellulosic biofuel supply chains: multiobjective optimization coupled with life cycle assessment and input–output analysis. AIChE J. 59 (4), 215–228.

Rangaiah, G., Sharma, S., Sreepathi, B.K., 2015. Multi-objective optimization for the design and operation of energy efficient chemical processes and power generation. Curr. Opin. Chem. Eng. 10, 49–62.

Sabio, N., Kostin, A., Guillén-Gosálbez, G., Jiménez, L., 2012. Holistic minimization of the life cycle environmental impact of hydrogen infrastructures using multi-objective optimization and principal component analysis. Int. J. Hydrog. Energy 37 (6), 5385–5405.

Sack, M., 2021. Implementation and Validation of a Multi Layer Model Predictive Controller for Energy Supply Systems. TU Wien.

Samsatli, S., Samsatli, N.J., 2018. A multi-objective MILP model for the design and operation of future integrated multi-vector energy networks capturing detailed spatio-temporal dependencies. Appl. Energy 220 (September 2017), 893–920.

Sankar Parhi, S., Rangaiah, G.P., Jana, A.K., 2020. Mixed-Integer dynamic optimization of conventional and vapor recompressed batch distillation for economic and environmental objectives. Chem. Eng. Res. Des. 154, 70–85.

Schmitt, T., Rodemann, T., Adamy, J., 2020. Multi-objective model predictive control for microgrids. At-Automatisierungstechnik 68 (8), 687–702.

B.V. Solanki, S. Member, K. Bhattacharya, and C.A. Canizares, "A sustainable energy management system for isolated microgrids," vol. 8, no. 4, pp. 1507–1517, 2017.

Tan, B., Chen, H., 2020. Multi-objective energy management of multiple microgrids under random electric vehicle charging. Energy 208, 118360.

Terlouw, T., AlSkaif, T., Bauer, C., van Sark, W., 2019. Multi-objective optimization of energy arbitrage in community energy storage systems using different battery technologies. Appl. Energy 239 (October 2018), 356–372.

Vadenbo, C., Hellweg, S., Guillén-Gosálbez, G., 2014. Multi-objective optimization of waste and resource management in industrial networks - Part I: model description. Resour. Conserv. Recycl. 89, 52–63.

Wang, J., Qiao, F., Zhao, F., Sutherland, J.W., 2016. Batch scheduling for minimal energy consumption and tardiness under uncertainties: a heat treatment application. CIRP Ann. Manuf. Technol. 65 (1), 17–20.

Wu, Q., Ren, H., Gao, W., Ren, J., 2016. Multi-objective optimization of a distributed energy network integrated with heating interchange. Energy 109, 353–364.

Yuan Qian, S., Hong Jia, Z., Li, K., 2020. A multi-objective evolutionary algorithm based on adaptive clustering for energy-aware batch scheduling problem. Future Gen. Comput. Syst. 113, 441–453.

Zavala, V.M., 2013. Real-time optimization strategies for building systems†. Ind. Eng. Chem. Res. 52 (9), 3137–3150.

Zhang, S., Zhuang, Y., Tao, R., Liu, L., Zhang, L., Du, J., 2020. Multi-objective optimization for the deployment of carbon capture utilization and storage supply chain considering economic and environmental performance. J. Clean. Prod. 270, 122481.

Zhong, Z., You, F., 2011. Oil spill response planning with consideration of physicochemical evolution of the oil slick: a multiobjective optimization approach. Comput. Chem. Eng. 35 (8), 1614–1630.

Zhou, S., Li, X., Du, N., Pang, Y., Chen, H., 2018. A multi-objective differential evolution algorithm for parallel batch processing machine scheduling considering electricity consumption cost. Comput. Oper. Res. 96, 55–68.